Tire *et al. Journal of Ovarian Research* (2025) 18:210
https://doi.org/10.1186/s13048-025-01735-x

Journal of Ovarian Research

RESEARCH Open Access

Superovulation alters telomere length and telomerase component levels in mouse oocytes

Betul Tire[1], Gunel Talibova[1], Yesim Bilmez[1] and Saffet Ozturk[1*]

Abstract

Assisted reproductive technologies (ARTs) are widely used to treat infertility and include the fundamental step, controlled ovarian stimulation (also known as superovulation). Superovulation involves the administration of gonadotropins to produce a sufficient number of oocytes, either through single or repeated applications. However, superovulation can cause certain adverse effects such as increased oxidative stress, decreased oocyte quality, and mitochondrial dysfunction. As oxidative stress and mitochondrial dysfunction are closely associated with alterations in telomere length, we investigated the effects of single and repeated superovulation on expression of the telomerase components and telomere length in mouse oocytes at germinal vesicle (GV) or metaphase II (MII) stage. Additionally, we measured serum levels of estradiol, progesterone, and oxidative markers. Our findings revealed that superovulation significantly affected telomere length, TERT protein level, telomerase RNA component (*Terc*), and telomerase reverse transcriptase (*Tert*) mRNA levels in these oocytes possibly due to altered estradiol and progesterone profiles ($P < 0.05$). These results suggest that altered telomerase expression and telomere length may contribute to emerging adverse effects of superovulation during oocyte maturation and early embryo development.

Keywords Superovulation, Mouse oocytes, Telomerase expression, Telomere length, Estradiol, Progesterone, Oxidative stress

Introduction

Superovulation, while increasing oocyte retrieval, can lead to reduced oocyte maturation rates [1, 2], delayed embryonic and fetal development [3, 4], abnormal blastocyst formation [4], and decreased implantation rates [2, 4]. On the other hand, repeated superovulation has been demonstrated to result in reduced oocyte quantity and quality [5], various morphological changes [2], abnormal meiotic spindles [4], altered genomic DNA methylation [6], increased oxidative stress [7, 8], and apoptosis [6] in mouse oocytes as well as changes in reproductive hormone levels and abnormal folliculogenesis [9, 10].

According to the literature analysis, the impact of superovulation on telomere biology remains poorly understood. Telomeres located at the ends of eukaryotic chromosomes are known to be evolutionarily conserved and non-coding repetitive DNA sequences (5'-TTAGGG-3')$_n$. This unique structure maintains genomic integrity throughout the lifespan. Telomeres are shortened by several factors, including DNA replication, oxidative stress, biological aging, and obesity [11, 12]. The short telomeres can be lengthened by the enzyme telomerase and the

*Correspondence:
Saffet Ozturk
sozturk@akdeniz.edu.tr
[1]Department of Histology and Embryology, Akdeniz University School of Medicine, Campus, Antalya 07070, Türkiye

© The Author(s) 2025. **Open Access** This article is licensed under a Creative Commons Attribution-NonCommercial-NoDerivatives 4.0 International License, which permits any non-commercial use, sharing, distribution and reproduction in any medium or format, as long as you give appropriate credit to the original author(s) and the source, provide a link to the Creative Commons licence, and indicate if you modified the licensed material. You do not have permission under this licence to share adapted material derived from this article or parts of it. The images or other third party material in this article are included in the article's Creative Commons licence, unless indicated otherwise in a credit line to the material. If material is not included in the article's Creative Commons licence and your intended use is not permitted by statutory regulation or exceeds the permitted use, you will need to obtain permission directly from the copyright holder. To view a copy of this licence, visit http://creativecommons.org/licenses/by-nc-nd/4.0/.

alternative lengthening of telomeres (ALT) mechanism. Telomerase is basically composed of two major subunits: the telomerase RNA component (*TERC*), which serves as an RNA template, and the catalytic subunit, telomerase reverse transcriptase (TERT). The telomerase activity has been determined in certain cell types, including germ cells, early embryos, and granulosa cells (Reviewed in [13, 14]).

The *Tert* gene expression, used as a biomarker of telomerase activity, is regulated by the reproductive hormones, estrogen and progesterone [15, 16]. In fact, estrogen binds to the estrogen response element (ERE) located in the *Tert* promoter region [17]. Estrogen is also able to enhance the *Tert* gene expression through elevating *c-Myc* transcript level [18]. As expected, estrogen deficiency leads to decreased TERT protein levels and thus telomerase activity in the mouse ovary [17]. In contrast, progesterone plays an inhibitory role in the human *TERT* gene expression and thereby telomerase activity, as demonstrated in the endometrial cells (reviewed in [15]). Similarly, while estrogen induces the *TERC* RNA level [15], progesterone has a suppressive effect on its level [19]. There is also an association between oxidative stress and subcellular distribution of TERT protein [20]. In other words, TERT protein not only plays a role in telomere elongation but also participates in the protection against oxidative stress by localizing into mitochondria [21]. Because superovulation can lead to increasing in oxidative stress in mouse oocytes [5, 22], its effect on TERT protein level and telomere length in these cells remains elusive.

Based on the literature review, a limited number of studies have examined the effects of superovulation on telomere length and expression of the telomerase components in mouse oocytes. In one such study by Mordechai et al., (2020), PMSG injection was reported to increase *Tert* mRNA and TERT protein levels, and telomerase activity in the rat granulosa cells [23]. In parallel with this study, Berteli et al., (2022) showed that blastocysts generated in vivo or in vitro after superovulation had higher telomere length than blastocysts generated in vivo from natural mating cycles [24]. In this study, we examined the *Tert* mRNA and *Terc* RNA levels in the mouse oocytes at germinal vesicle (GV) or metaphase II (MII) stage. Additionally, we assessed the subcellular localization of TERT protein and measured telomere length. Serum estradiol and progesterone levels as well as oxidant and antioxidant status were also determined.

Materials and methods

Animals and sample collection

The female (9–13 weeks old, $n = 160$) and vasectomized male (8 weeks old, $n = 6$) Balb/C mice were provided by the Experimental Animals Application and Research Center of Akdeniz University. These mice were kept under a 12 h light/12 h dark cycle with no water or food restriction. All procedures followed the guidelines and regulations approved by the Institutional Animal Care and Use Committee of Akdeniz University (protocol no. 1312/2021.05.24). Also, all methods were performed in accordance with the ARRIVE guidelines.

The estrous cycles of all female mice were determined by taking daily vaginal smears, evaluated under bright-field microscopy after stained with 1% toluidine blue (Supplementary Fig. 1). Mice in diestrous phase were included [7] in creating the four groups: Control (C; $n = 13$ for GV and $n = 32$ for MII oocyte collection), once superovulated (1S; $n = 12$ for GV and $n = 24$ for MII oocyte collection), three times superovulated (3S; $n = 18$ for GV and $n = 25$ for MII oocyte collection), and five times superovulated (5S; $n = 14$ for GV and $n = 22$ for MII oocyte collection) at 1-week intervals (Fig. 1), as used in previous investigations [9, 25].

In the superovulated groups, GV oocytes were collected from dissected ovaries 44 h after an intraperitoneal injection of 8 international units (IU) of pregnant mare serum gonadotropin (PMSG; catalog no. 182779R1, MSD Animal Health, New Jersey, USA) each time. The cumulus oocyte complexes (COCs) including MII oocytes were obtained from the oviducts of mice undergoing intraperitoneal injection of 8 IU PMSG, followed 48 h later by injection of 8 IU of human chorionic gonadotropin (hCG, catalog no.194225R2, MSD Animal Health) each time.

As was performed in the 5S group for gonadotropin injections, control mice were administered five injections of sterile water intraperitoneally at 1-week intervals to avoid possible confounding factors such as injection-induced stress. All injections were made every week on the same day at 5:00 pm. The injections started at 9–11 weeks of age in the control and 5S groups, and at 11–13 and 13–15 weeks of age in the 3S and 1S groups, respectively. It is worth noting that no additional water injections were performed to the 1S and 3S groups. All mice were euthanized by the cardiac puncture method under anesthesia that was induced by intraperitoneal injection of a cocktail of ketamine (100 mg/kg) and xylazine (10 mg/kg) at 13–15 weeks of age.

The control GV oocytes were collected from naturally cycling females. For COCs collection, control mice were randomly mated with vasectomized male Balb/C mice and checked for the presence of a vaginal plug at 8:00 am. As it was performed in the superovulated groups, COCs obtained from control mice were incubated with 1 mg/mL hyaluronidase (catalog no. 37326-33-3, Sigma-Aldrich, St. Louis, MO, USA) in Dulbecco's modified Eagle's medium (DMEM): F12 (Gibco, Life Sciences) to remove cumulus cells.

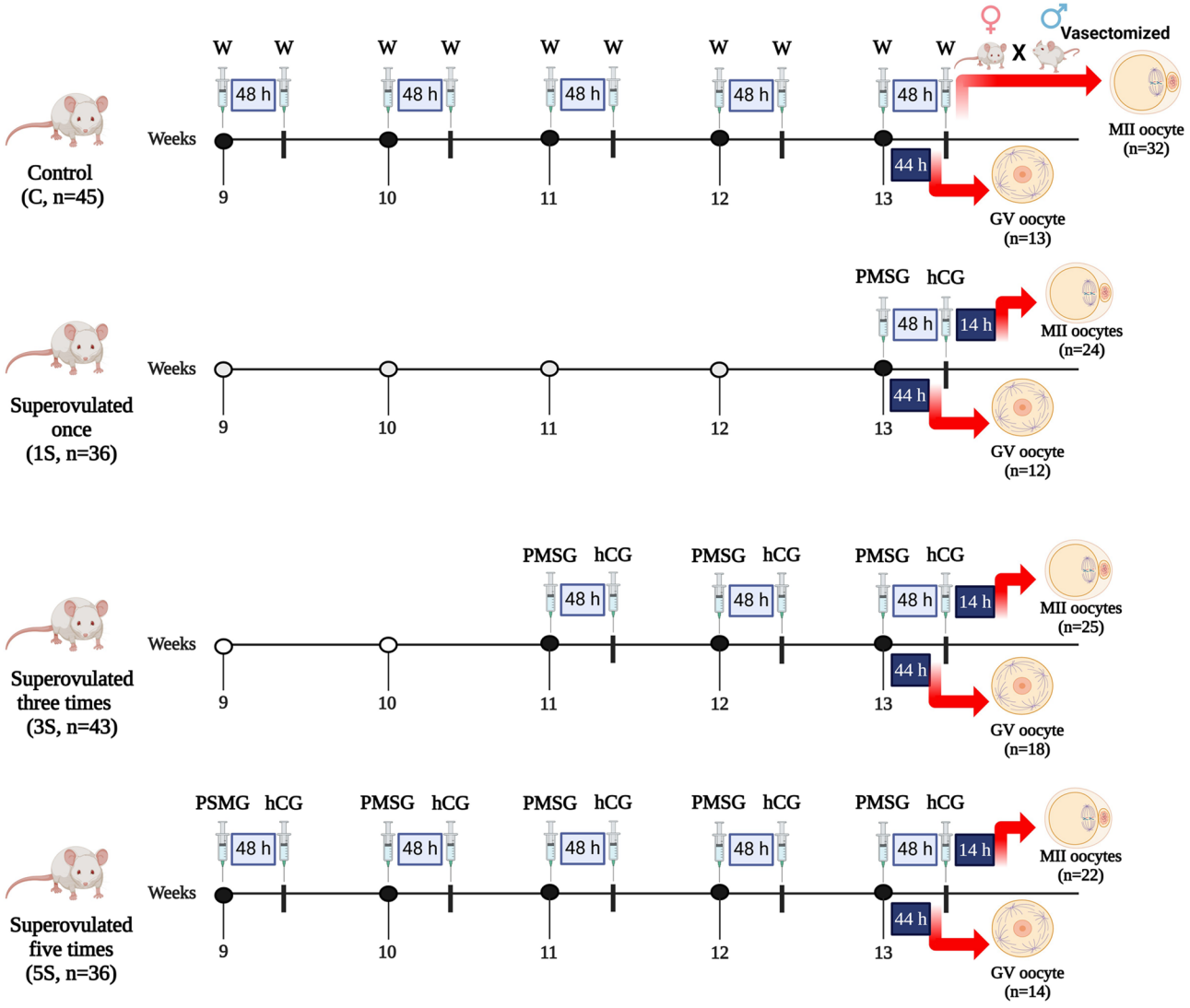


Fig. 1 Experimental model of this study to obtain germinal vesicle (GV) and metaphase II (MII) oocytes from the control and superovulated groups. Superovulation was induced by intraperitoneal injection of 8 IU pregnant mare serum gonadotropin (PMSG), followed 48 h later by 8 IU human chorionic gonadotropin (hCG). GV oocytes were collected from ovaries 44 h after PMSG injection, while MII oocytes were collected from the oviducts 14–16 h after hCG injection. Based on these injections, we formed the following four groups: Control (C; $n=13$ for GV and $n=32$ for MII oocytes collection), once superovulated (1S; $n=12$ for GV and $n=24$ for MII oocytes collection), three times superovulated (3S; $n=18$ for GV and $n=25$ for MII oocytes collection) at 1-week intervals and five times superovulated (5S; $n=14$ for GV and $n=22$ for MII oocytes collection) at 1-week intervals. It is worth noting that we injected water to control mice five times at one-week intervals. Additionally, MII oocytes from control group were obtained following mating with vasectomized males. Furthermore, all mice were of the same age at the time they were included in the experiment. The GV and MII oocytes collected from the control and superovulated groups were used in related experiments. W, water. This figure was created using the BioRender program (BioRender Inc., Toronto, Canada)

In both control and superovulated groups, only GV and MII oocytes showing normal morphological appearance with respect to cytoplasmic granulation, perivitelline space, and zona pellucida thickness were utilized in the subsequent experiments, while oocytes with abnormal morphology, large perivitelline space, cytoplasmic granulation, and thick zona pellucida were excluded [26, 27]. We employed qPCR to measure telomere length, immunofluorescence to determine subcellular localization of TERT protein and real time-quantitative polymerase chain reaction (RT-qPCR) to assess the *Terc* RNA and *Tert* mRNA levels.

In addition to oocyte collections, blood samples of mice were collected using the cardiac puncture method [12, 28]. Blood samples were then centrifuged at 3.000 rpm for 15 min. The obtained serum samples were stored at -80 °C until further analysis for total oxidant status (TOS), total antioxidant status (TAS), and ELISA to measure estradiol and progesterone levels.

Table 1 The primer sequences of telomere and *mB1* gene

Gene	Primer (5′➔3′)
Telomere	P_F:CGGTTTGTTTGGGTTTGGGTTTGGGTTTGGGTTTGGGTT
	P_R: GGCTTGCCTTACCCTTACCCTTACCCTTACCCTTACCCT
mB1	P_F: GCACCTTTAATCCCAGCAC
	P_R: TGAGACAGGGTTTCTCTGTA

P_F, forward primer; P_R, reverse primer

Telomere length analysis

Telomere length was determined in GV ($n=6$ mice, with a pool of at least 50 oocytes per group) and MII oocytes (C, $n=20$; 1S, $n=14$; 3S, $n=13$; and 5S, $n=15$ mice, with a pool of at least 50 oocytes per group) using the conventional qPCR method as described in previous studies [24, 29, 30]. The genomic DNA was extracted from these oocytes using QIAmp DNA Micro kit (catalog no. 56304, Qiagen, Valencia, CA, USA). Genomic DNA concentration and absorbance were measured using the Epoch Microplate (BioTek Instruments, Inc., Charlotte, VT, USA). The mouse B1 retrotransposon (*mB1)* served as a reference in the qPCR analysis for telomere length measurement [24]. The primer sequences are presented in Table 1. The qPCR reactions were performed in triplicate for each group. Melting curve analysis was also used to verify specificity of the qPCR products. The relative telomere length for each group was calculated using the $2^{-\Delta\Delta Ct}$ formula, where Ct represents cycle threshold.

Immunofluorescence staining

As described in our previous studies [31, 32], immunofluorescence staining was used to determine intracellular localization and relative levels of TERT protein in GV and MII oocytes from both control and superovulated groups. At least 3 oocytes per mouse ($n=6$, a minimum of 18 oocytes analyzed for each group) were stained. We utilized polyclonal primary TERT antibody (diluted at 1:400 in antibody diluent; catalog no. bs-0233R, Bioss Inc., Woburn, MA, USA) and isotype control IgG antibody (catalog no. I5006, Sigma-Aldrich) to confirm specificity of the primary antibody. The secondary anti-rabbit Alexa fluor® 488 antibody (diluted 1:2000; catalog no. 4412S, Cell Signaling Technology, Danvers, MA, USA) was used. The immunostained oocytes were examined under a fluorescence microscope (Olympus BX61, Tokyo, Japan) at 400× magnification. As in previous studies [29, 31], the relative TERT protein levels were measured in the total, nuclear, and cytoplasmic areas of GV oocytes, as well as in the total and polar bodies of MII oocytes using the ImageJ software program (National Institutes of Health, Bethesda, Maryland, USA).

Gene expression analysis

Total RNA was extracted from at least 50 GV (C, $n=6$; 1S, $n=6$; 3S, $n=8$; 5S, $n=7$ mice) and MII oocytes (C, $n=21$; 1S, $n=11$; 3S, $n=13$, and 5S, $n=13$ mice) using RNAqueous-Micro kit (Ambion Inc., Austin, Texas, USA). The DNase kit from Ambion Inc. was utilized to remove any potential contamination from genomic DNA. Complementary DNA (cDNA) was then synthesized using RETROscript Reverse Transcription kit (Ambion Inc.) by utilizing random decamer primers according to the manufacturer's instructions.

Table 2 The primer sequences and product sizes of the *Tert*, *Terc*, and *β-Act* genes used in real time-quantitative polymerase chain reaction (RT-qPCR)

Gene	Primers (5′➔3′)	Product size (bp)
Tert	P_F: CTCTCTGCTGCGCAGCCGATAC	287
	P_R: CCTCGTTAAGCAGCTCAAAG	
Terc	P_F: CATTAGCTGTGGGTTCTGGTCT	134
	P_R: TCCTGCGCTGACGTTTGTTT	
β-Act	P_F: TGCGTGACATCAAAGAGAAG	244
	P_R: CGGATGTCAACGTCACACTT	

β-Act, beta actin; *Tert*, telomerase reverse transcriptase; *Terc*, telomerase RNA component; P_F, forward primer; P_R, reverse primer; bp, base pair

As in our previous studies [33–35], RT-qPCR was performed on a Rotor-Gene instrument (Corbett Research, Sydney, Australia) using the same thermal cycler reaction conditions after setting up the reaction tubes. The primer sequences and product sizes are presented in Table 2. The beta-actin (*β-Act*) mRNA levels were used as an internal control to normalize the *Terc* and *Tert* transcript levels. The relative transcript levels for each gene were calculated using the $2^{-\Delta\Delta Ct}$ formula, where Ct represents cycle threshold. It is crucial to emphasize that the term "relative" pertains to a ratio of measured target transcript level to transcript level of reference gene, *β-Act*. RT-qPCR reactions were performed in triplicate for each group.

Measurement of reproductive hormones

The estradiol and progesterone levels were measured in the serum samples obtained from the control and superovulated groups ($n=6$ mice per group) using the ELISA kits (E-OSEL-M0008 for estradiol and E-OSEL-M0006 for progesterone, Elabscience®, Texas, USA) according to the manufacturer's instructions. The estradiol [$y=-0.452\ln(x)+2.9791$, ($R^2=0.98$)] and progesterone [$y=-0.468\ln(x)+1.7625$ ($R^2=0.98$)] levels were calculated using the logarithmic curve formulas derived from their standard values.

Measurement of total oxidant and antioxidant status

The levels of TOS and TAS were determined in the serum samples obtained from the control and superovulated groups ($n=6$ mice per group) using specific kits (catalog no. E-BC-K801-M for TOS and catalog no. E-BC-K802-M for TAS, Elabscience®), as explained in the manufacturer's instructions. The TOS [$y=0.0007x$

- 0.0031 (R^2=0.99)] and TAS [y = 0.1276x - 0.0982 (R^2=0.99)] levels were calculated using the logarithmic curve formulas derived from their standard values. The oxidative stress index (OSI) was determined as ratio of TOS to TAS levels [36].

Statistics

The obtained data are expressed as the mean ± standard deviation (SD). We evaluated the RT-qPCR, immunofluorescence, and qPCR data as well as the TAS, TOS, and OSI values by one-way ANOVA and Tukey's post hoc test. In the ELISA tests conducted for the purpose of assessing levels of estradiol and progesterone, an unpaired *t*-test was employed. The relationship between the levels of *Tert* mRNA, TERT protein, *Terc* RNA, and telomere length were evaluated using Pearson's correlation test. All statistical calculations were performed using GraphPad Prism 5 software (GraphPad Software Inc., San Diego, CA, USA). $P < 0.05$ was considered statistically significant.

Results

In this study, we investigated the effects of superovulation on telomere length, *Tert* mRNA and *Terc* RNA levels in the GV and MII stage oocytes as well as on estradiol and progesterone concentrations, TAS, TOS, and OSI levels in serum samples of the control and superovulated mice.

Ovarian structure and retrieved oocyte counts in the control and superovulated groups

We initially examined the effects of superovulation on ovarian structure. The GV and MII oocyte-collected superovulation groups exhibited a greater prevalence of corpus lutea and fewer growing follicles when compared to controls (Supplementary Fig. 2A). Interestingly, polyovular follicles (POFs) [37] were exclusively observed in the ovaries of GV oocyte-collected superovulated groups (Supplementary Fig. 2B).

The normal and abnormal numbers and percentages of GV and MII oocytes were provided for each group (Table 3). The percentages of normal and abnormal GV oocytes in the 1S and 3S groups were found to be comparable to those of control group. However, the 5S group exhibited a lower percentage of normal GV oocytes and a higher percentage of abnormal GV oocytes when compared to the other groups. In MII oocytes, the superovulated groups (1S, 3S, and 5S) exhibited lower normal percentages and higher abnormal percentages when compared to control group (Table 3).

Telomere length in GV and MII oocytes

We determined telomere length in the GV and MII oocytes, obtained from control and superovulated groups. Telomere length in GV oocytes decreased significantly in the superovulated groups (1S, 3S, and 5S) compared to control group ($P < 0.001$; Fig. 2A). In MII oocytes, telomere length increased dramatically in the 1S group ($P < 0.001$) in comparison to control group, then decreased in the 3S group ($P < 0.001$), and finally increased again in the 5S group ($P < 0.001$; Fig. 2B). It is noteworthy that MII oocytes of the 1S and 5S groups had the highest telomere length ($P < 0.001$).

TERT protein levels in GV and MII oocytes

The intracellular localization and relative levels of TERT protein in GV oocytes (Fig. 3), MII oocytes and their first polar bodies (Fig. 4) were examined in control and superovulated groups. In GV oocytes, it was highly localized in the nucleus and less in the cytoplasm of both control and superovulated groups (Fig. 3A). When analyzing the relative levels of TERT protein in total (Fig. 3B), nuclear (Fig. 3C), and cytoplasmic (Fig. 3D) area of GV oocytes, we found no significant changes between the groups despite minor variations.

We observed strong TERT protein intensity in the cytoplasmic region of MII oocytes and their first polar bodies, but a weak intensity in the nuclear region of MII oocytes (Fig. 4). The total TERT protein level in MII

Table 3 The numbers of mice, normal and abnormal oocytes, and the average numbers (percentages) of oocytes at GV or MII stage, collected per mouse for all groups

	Group	Number of normal oocytes	Number of mice	Average number of normal oocytes per mouse (Ratio of normal oocytes to total oocytes)	Number of abnormal oocytes	Number of mice	Average number of abnormal oocytes per mouse (Ratio of normal oocytes to total oocytes)
GV Oocytes	**C**	237	13	18.23 **(88.1%)**	32	4	8.0 **(11.9%)**
	1S	293	12	24.41 **(88.3%)**	39	6	6.5 **(11.7%)**
	3S	336	18	18.66 **(87.5%)**	48	7	6.8 **(12.5%)**
	5S	242	14	17.28 **(82.6%)**	51	8	6.3 **(17.4%)**
MII Oocytes	**C**	142	32	4.43 **(83.5%)**	28	7	4.0 **(16.5%)**
	1S	213	24	8.87 **(50.5%)**	209	15	13.9 **(49.5%)**
	3S	167	25	6.68 **(53.2%)**	147	15	9.8 **(46.8%)**
	5S	182	22	8.27 **(48.0%)**	197	14	14.07 **(52.0%)**

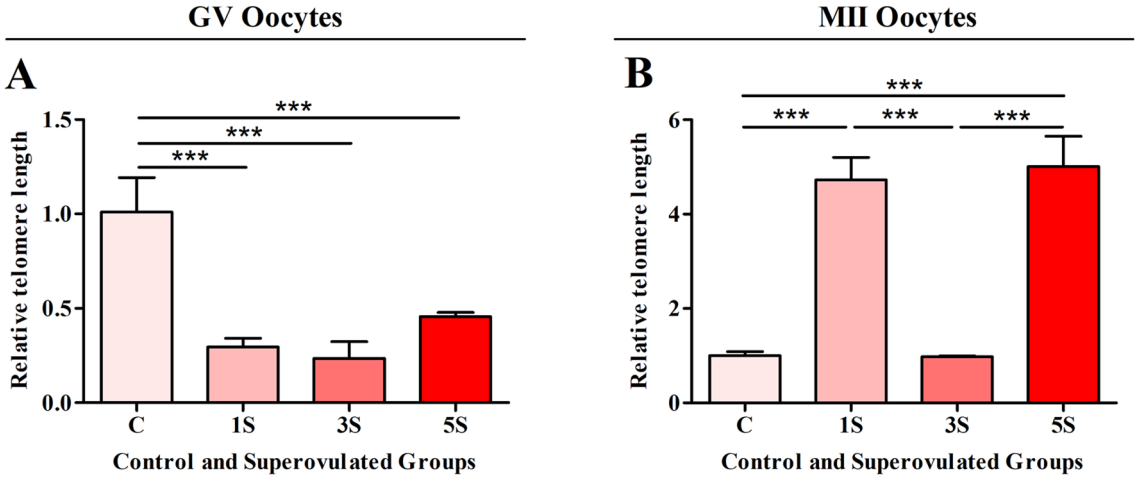


Fig. 2 The relative telomere length in GV and MII oocytes of the control and superovulated groups. (**A**) The relative telomere length in GV oocytes. It significantly decreased in the 1S, 3S, and 5S groups compared to control group ($P < 0.001$). (**B**) The relative telomere length in MII oocytes. It reached the highest levels in the 1S and 5S groups but was the lowest in the 3S group ($P < 0.001$). For qPCR analysis, GV oocytes were collected from 6 mice and pooled to create a minimum of 50 oocytes per group ($n = 6$). MII oocytes were collected from the control and superovulated groups (C, $n = 20$; 1S, $n = 14$; 3S, $n = 13$; and 5S, $n = 15$ mice) and at least 50 oocytes were pooled per group. The statistical calculations were performed using one-way ANOVA and Tukey's post hoc test. Data are presented as mean ± standard deviation (SD). $P < 0.05$ was considered statistically significant. Asterisks indicate significant difference, ***$P < 0.001$. C, control; S, superovulated

oocytes significantly increased from control to the 5S groups ($P < 0.05$; Fig. 4B). Similarly, TERT levels in the first polar bodies of MII oocytes increased from control to the 5S groups ($P < 0.05$; Fig. 4C).

***Terc* RNA and *Tert* mRNA levels in GV and MII oocytes**.

In control and superovulated groups, we first examined the levels of *Terc* RNA and *Tert* mRNA in GV and MII oocytes (Fig. 5). Although the relative *Terc* RNA levels were comparable among control, 1S, and 3S groups, it increased in the 5S group (Fig. 5A). However, we only found a significant difference between the 1S and 5S groups ($P < 0.05$). In MII oocytes, the *Terc* RNA levels increased from control to the 1S groups and then decreased dramatically in the 3S group ($P < 0.01$), finally increased again in the 5S group ($P < 0.01$; Fig. 5B).

The relative *Tert* mRNA levels of GV oocytes in control group increased in the 1S group, then decreased in the 3S group, and increased again in the 5S group (Fig. 5C). In other words, the 1S and 5S groups had higher *Tert* mRNA levels than control groups ($P < 0.05$). Although the *Tert* mRNA levels were similar in control, 3S, and 5S groups, it reached the highest level in the 1S group ($P < 0.001$; Fig. 5D).

Estradiol and progesterone levels in serum samples

We measured estradiol and progesterone levels in the serum samples of control and superovulated groups from which GV or MII oocytes were collected. The estradiol levels in mice from which GV oocytes were collected significantly increased in the superovulated groups (1S, 3S, and 5S groups) compared to control group ($P < 0.01$; Fig. 6A). In MII oocyte-collected groups, it decreased progressively from control to the 5S groups (Fig. 6B). It is important to note that the 3S and 5S groups possessed higher estradiol levels than control group ($P < 0.01$).

Progesterone levels increased progressively from control to the 5S groups in GV oocyte-collected mice (Fig. 6C). In other words, all superovulated groups (1S, 3S, and 5S groups) had significantly higher progesterone levels than control group ($P < 0.01$). In MII oocyte-collected mice, we found higher progesterone levels in the 1S, 3S, and 5S groups than in control group ($P < 0.001$), while no significant change was observed between the superovulated groups (Fig. 6D).

Analysis of TOS, TAS, and OSI in serum samples

We measured TAS and TOS levels in the serum samples of control and superovulated groups and also calculated OSI values. We found no significant changes in TOS levels in the mice from which GV and MII oocytes were collected (Fig. 7A and B). No significant changes were detected in TAS levels (Fig. 7C and D) and OSI values (Fig. 7E and F) between the groups.

Discussion

In the present study, we found that superovulation altered transcript levels of the *Terc* and *Tert* genes, TERT protein levels, and telomere length in GV and MII oocytes. Although superovulation does not affect TOS, TAS, and OSI levels, a notable elevation was determined in estradiol and progesterone levels in serum samples from superovulated mice, in comparison to the control group.

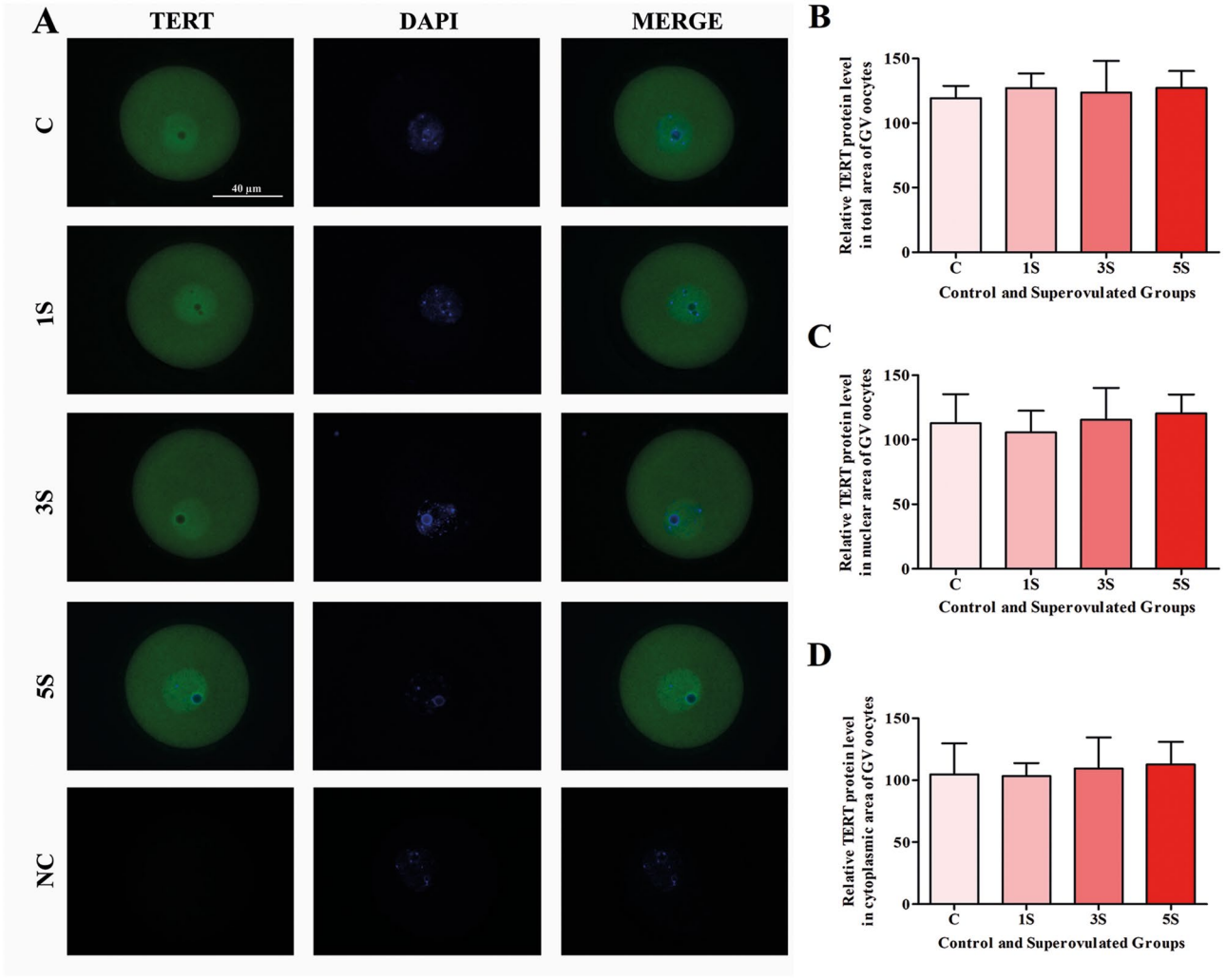


Fig. 3 The subcellular localization and relative levels of TERT protein in GV oocytes of the control and superovulated groups. (**A**) Subcellular localization of TERT protein. It was predominantly located in the nucleus and to a lesser extent in the cytoplasm. The micrographs were captured at 400× original magnification. The scale bars represent 40 µm. (**B**) The relative TERT levels in the total area of GV oocytes. We found no statistical significance among the groups. (**C**) The relative TERT level in the nuclear area of GV oocytes. No changes were observed between the groups. (**D**) The relative TERT level in the cytoplasmic area of GV oocytes. We observed no difference between the groups. At least 3 oocytes were stained per mouse ($n=6$), resulting in analysis of a minimum of 18 oocytes for immunofluorescence in each group. The statistical calculations were performed using one-way ANOVA and Tukey's post hoc test. Data are presented as mean ± standard deviation (SD). $P<0.05$ was considered statistically significant. C, control; S, superovulated; NC, negative control

It was observed that GV oocytes of the superovulated groups exhibited shorter telomeres than those of control group. However, no correlation was identified between the *Tert* mRNA, *Terc* RNA, and TERT protein levels and the telomere length. These oocytes showed an upregulation of *Tert* mRNA levels, likely due to elevated estradiol and progesterone concentrations [15, 17]. Also, shortening of telomere length due to superovulation may increase transcript levels of the *Tert* and *Terc* genes by a mechanism that is currently unknown. Thus, TERT protein level and thereby telomerase activity were intended to increase, but no significant change was observed in TERT protein levels. This discrepancy may be attributed to post-transcriptional control mechanism, which may regulate TERT protein level during developmental periods.

The differences in numbers of GV and MII oocytes in the control and superovulated groups suggest that a significant proportion of GV oocytes were incapable of completing meiotic maturation. Insufficiencies of gonadotropins, FSH and LH, and their receptors as well as defects in cytoplasmic and nuclear maturation and impaired ovulation process may lead to disrupting meiotic completion in most GV oocytes. On the other hand, higher numbers of abnormal GV and MII oocytes in the superovulated groups compared to control group suggest that although treatment with gonadotropins contributed to stimulating meiotic division [38], these hormones may

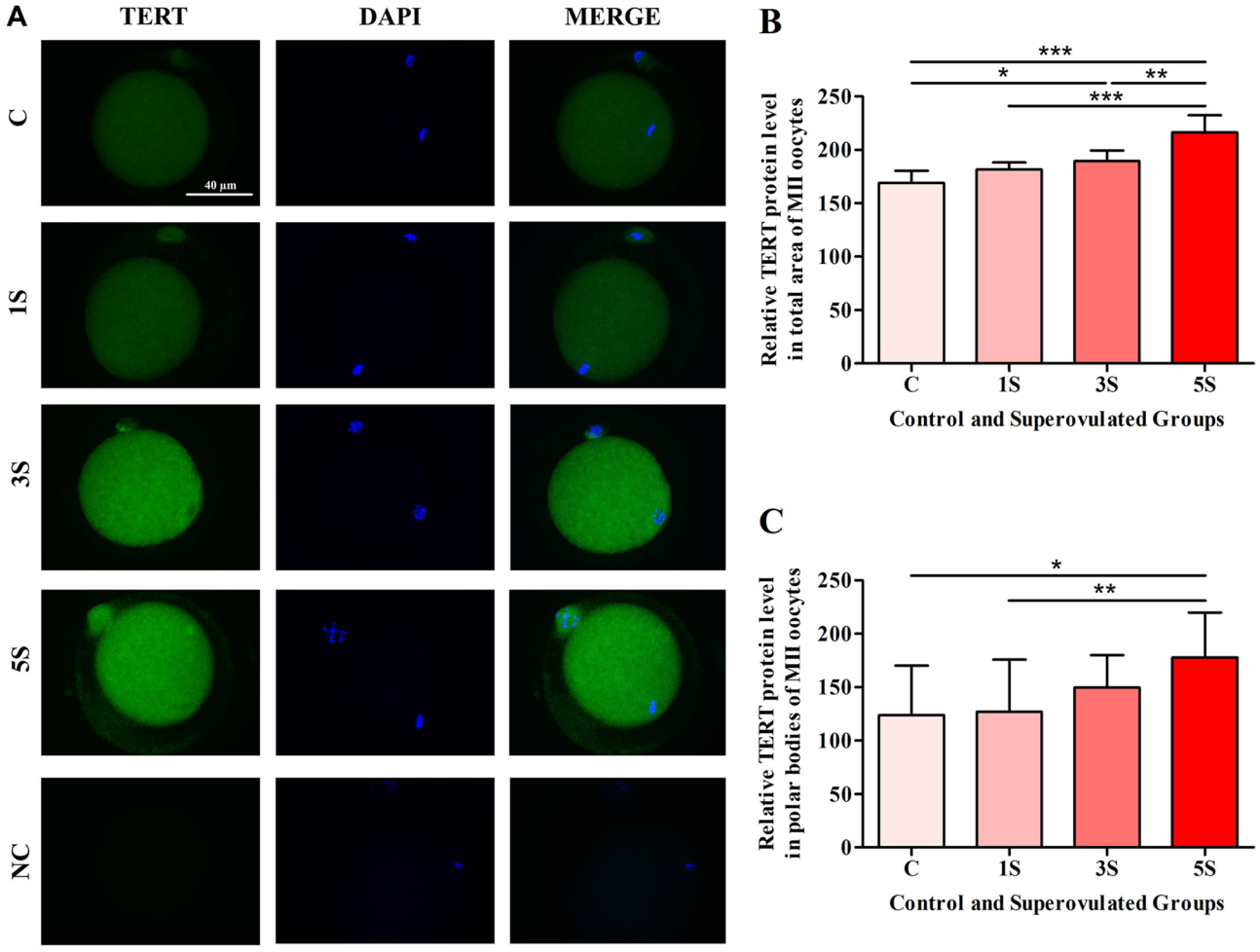


Fig. 4 The subcellular localization and relative levels of TERT protein in MII oocytes and their polar bodies of the control and superovulated groups. (**A**) Subcellular localization of TERT protein. It was strongly expressed in MII oocytes and their polar bodies, but there was weak staining in the nuclear region of MII oocytes. The micrographs were captured at 400× original magnification. The scale bars represent 40 µm. (**B**) The relative TERT levels in the total area of MII oocytes. We found a gradual increase from control to the 5S groups ($P < 0.05$). (**C**) The relative TERT levels in the polar bodies. Similar to MII oocytes, polar bodies showed gradually increasing levels from control to the 5S groups ($P < 0.05$). At least 3 oocytes were stained per mouse ($n = 6$), resulting in analysis of a minimum of 18 oocytes for immunofluorescence in each group. The statistical calculations were performed using one-way ANOVA and Tukey's post hoc test. Data are presented as mean ± standard deviation (SD). $P < 0.05$ was considered statistically significant. Asterisk(s) indicate significant differences as follows: *$P < 0.05$, **$P < 0.01$, ***$P < 0.001$. C, control; S, superovulated; NC, negative control

be unable to provide normal oocyte growing and maturation. Additionally, gonadotropins may cause the development of follicles that would not develop under normal conditions [39]. This issue can result in production and ovulation of oocytes including some morphological abnormalities.

Increased oxidative stress caused by superovulation in ovarian microenvironment [22] may also cause telomere shortening in GV oocytes. As is known, DNA breaks and modified bases such as 8-oxoguanine formed by excess oxidative stress are repaired by DNA double strand break (DSB) repair and base excision repair (BER) mechanisms [12, 40]. These repair mechanisms may result in a partial shortening of telomeres in GV oocytes, which should be examined in future studies.

In MII oocytes, telomere length has demonstrated fluctuations between the superovulated groups, exhibiting no correlation with *Tert* mRNA and TERT protein levels. Interestingly, a positive correlation was observed between telomere length and *Terc* RNA levels (Supplementary Fig. 3). Given that *Terc* acts as an RNA template for telomerase activity, it might be a limiting factor for telomere elongation in MII oocytes as both parameters showed similar changes among the groups. Thus, regulation of *Terc* expression in the context of repeated superovulation remains unclear and warrants further investigation. It is likely that *Terc* RNA may have roles other than its known basic role in telomere length control. Ovarian steroid hormones, particularly estrogen and progesterone, have been shown to modulate expression

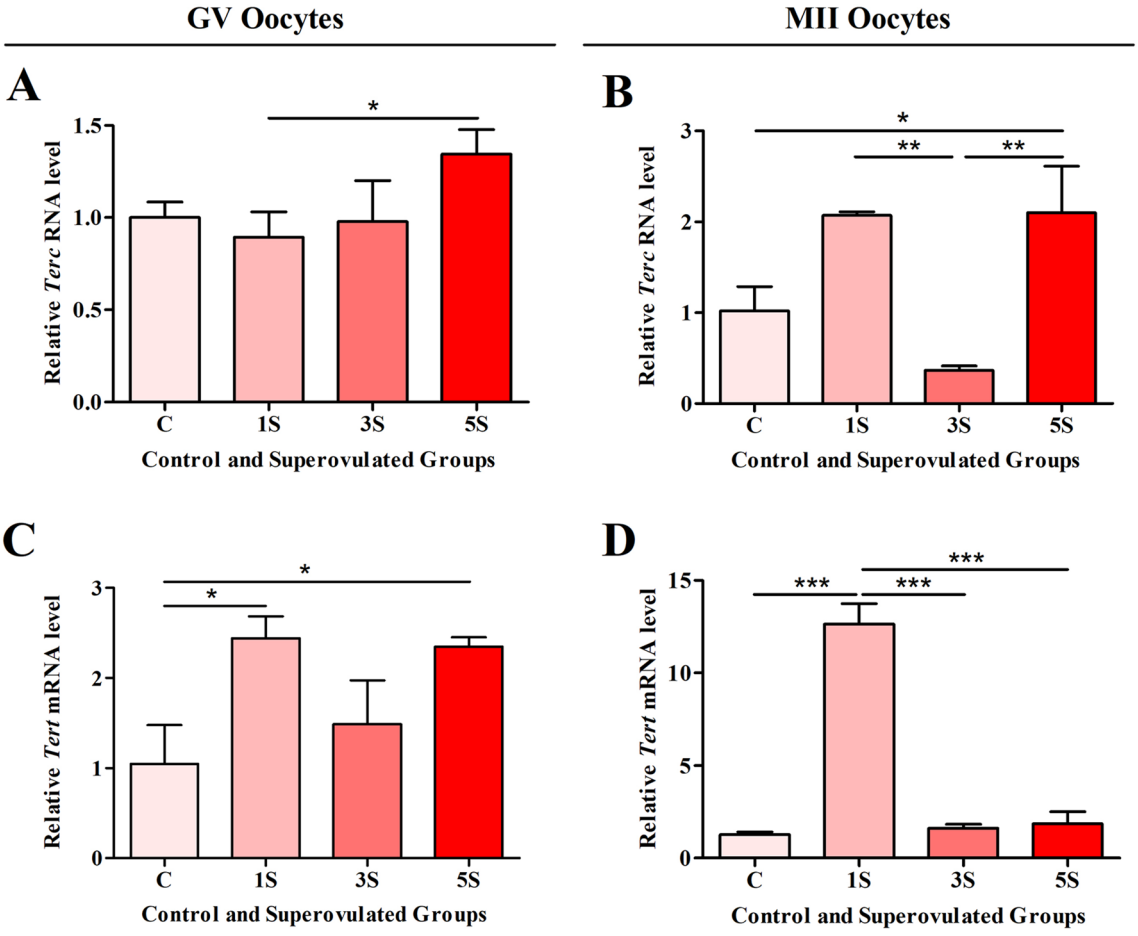


Fig. 5 The relative levels of *Terc* RNA and *Tert* mRNA levels in GV and MII oocytes of the control and superovulated groups. (**A**) The relative *Terc* RNA levels in GV oocytes. Its level in GV oocytes of the 5S group was significantly higher than that of the 1S group ($P < 0.05$). (**B**) The relative *Terc* RNA levels in MII oocytes. It was at the lowest level in the 3S group ($P < 0.01$). (**C**) The relative *Tert* mRNA levels in GV oocytes. The 1S and 5S groups had higher levels than control group. (**D**) The relative *Tert* mRNA levels in MII oocytes. It reached the highest level in the 1S group ($P < 0.001$). For RT-qPCR analysis, GV oocytes were collected from control and superovulated groups (C, $n = 6$; 1S, $n = 6$; 3S, $n = 8$; 5S, $n = 7$) and pooled to create a minimum of 50 oocytes per group. Similarly, MII oocytes were collected from control and superovulated groups (C, $n = 21$; 1S, $n = 11$; 3S, $n = 13$; and 5S, $n = 13$) and pooled to create a minimum of 50 oocytes per group. The statistical calculations were performed using one-way ANOVA and Tukey's post hoc test. Data are presented as mean ± standard deviation (SD). $P < 0.05$ was considered statistically significant. The asterisk(s) indicate significant differences as follows: $^{*}P < 0.05$, $^{**}P < 0.01$, and $^{***}P < 0.001$. C, control; S, superovulated

of the telomerase components [15, 17]. Several studies have shown that estrogen deficiency is associated with decreased *Tert* gene expression, indicating that estrogen may play a regulatory role in controlling its expression [17, 41, 42]. A decrease in estrogen levels, as observed in the 3 S group, may have contributed to downregulating *Tert* mRNA expression. In parallel, reduced levels of *Terc* RNA may have further limited telomerase activity, collectively resulting in telomere shortening in the 3 S group.

A review article highlighted that progesterone could also modulate telomerase activity, supporting the involvement of both hormones in this regulatory network [15]. Therefore, it is plausible that hormonal fluctuations induced by repeated superovulation contributed to altered telomerase-related gene expression observed in the GV or MII oocytes. Nevertheless, further mechanistic studies are required to fully elucidate the molecular pathways involved in the regulation of telomere length by the actions of progesterone.

The augmented telomere length in MII oocytes of the superovulated groups may be reflected in subsequent embryonic stages. In a recent work by Berteli et al., (2022) reported that superovulation increased telomere length in the mouse blastocysts [24]. As a single dose superovulation had been used in this study, telomere elongation in these blastocysts may result from inherited long telomeres in MII oocytes.

As in our previous studies [31, 43], TERT protein was localized in both nuclear and cytoplasmic regions of GV and MII oocytes. In addition, it was observed in the first polar bodies of MII oocytes. TERT not only has a role in telomere elongation but also resides in mitochondria,

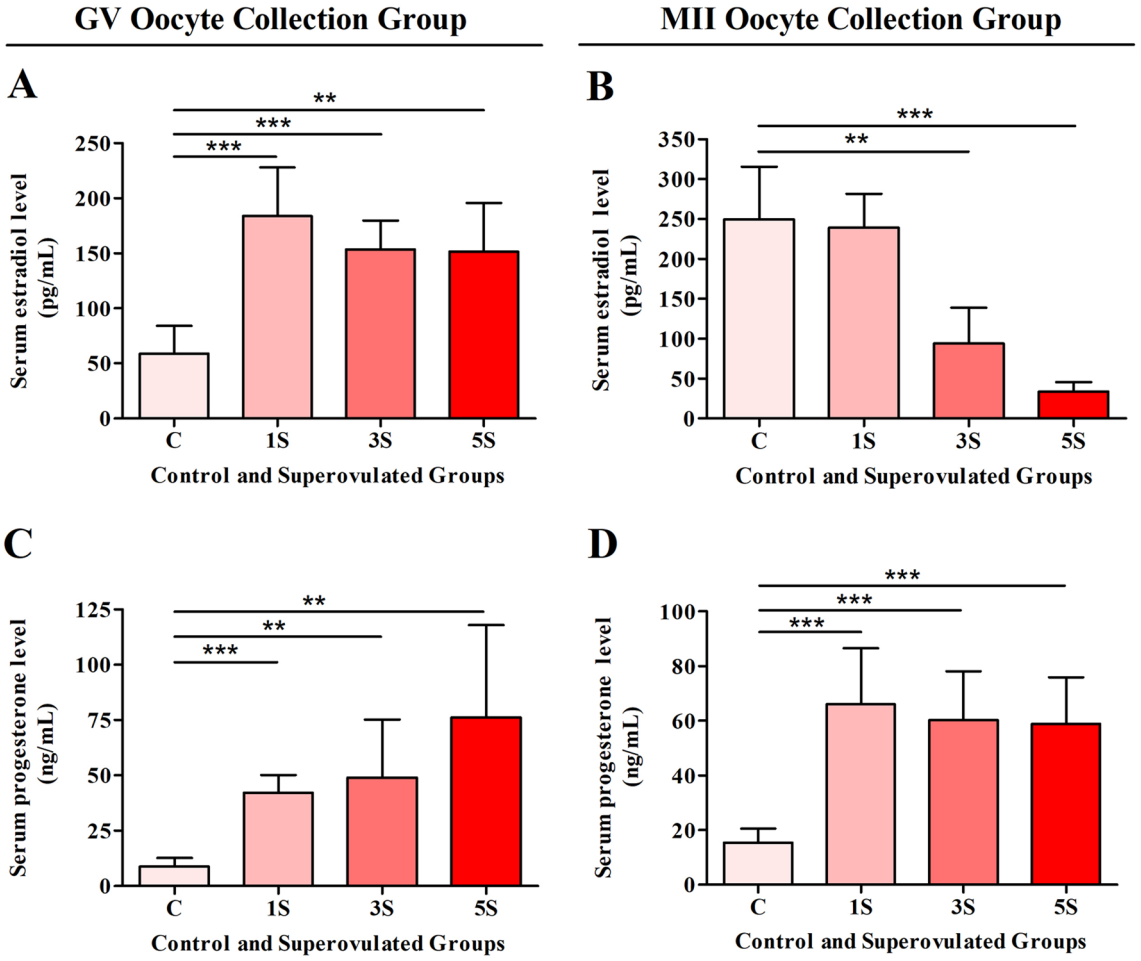


Fig. 6 The concentrations of estradiol and progesterone hormones in serum samples of GV- and MII-oocyte collected control and superovulated groups. (**A**) The estradiol concentrations in GV oocyte-collected groups. It dramatically increased in the superovulated groups (1S, 3S, and 5S; $P < 0.01$). (**B**) The estradiol concentrations in MII oocyte-collected groups. The 3S and 5S groups had lower levels compared to control group ($P < 0.01$). (**C**) The progesterone concentrations in GV oocyte-collected groups. It showed a gradual increase from the 1S to 5S groups when compared to control group ($P < 0.01$). (**D**) The progesterone concentrations in MII oocyte-collected groups. We found higher levels in the superovulated groups (1S, 3S, and 5S) than in control group ($P < 0.001$). Differences were analyzed by unpaired *t*-test when comparing the superovulated and control groups. Data are presented as mean ± standard deviation (SD). $P < 0.05$ was considered statistically significant. Asterisks indicate significant differences as follows: $^{**}P < 0.01$, $^{***}P < 0.001$. C, control; S, superovulated

considered a non-canonical role to protect this organelle from oxidative stress [20]. Therefore, subcellular distribution of TERT protein is consistent with its primary functions.

Although we found no significant changes in the oxidative stress levels in serum samples of the control and superovulated groups, two studies demonstrated that repeated superovulation increases oxidative stress in the oocytes and ovaries [5, 44]. The absence of significant changes in serum oxidative stress levels may be attributed to systemic antioxidant defense mechanisms that neutralize the effects of localized oxidative stress. This situation suggests that serum analyses may not fully reflect local oxidative stress conditions in ovarian microenvironment or oocytes themselves. The increased oxidative stress in ovarian microenvironment due to superovulation may cause elevated TERT protein levels in MII oocytes. Specifically, TERT levels in MII oocytes gradually increased from the 1S to 5S groups, potentially due to increased *Tert* mRNA levels immediately after superovulation. Although *Tert* mRNA levels decreased in the 3S and 5S groups possibly by post-transcriptional control mechanisms, the sustained increase in TERT protein levels is believed to result from initially produced mRNAs at the first superovulation, which may be sufficient to support ongoing protein synthesis. While we observed an increase in TERT protein levels in MII oocytes of the superovulated groups, no predominant changes were detected in GV oocytes among the groups. A significant increase in *Tert* mRNA levels of GV oocytes in the 1S and 5S groups showed that PMSG upregulates *Tert* gene transcription, but this increase was brought to normal levels

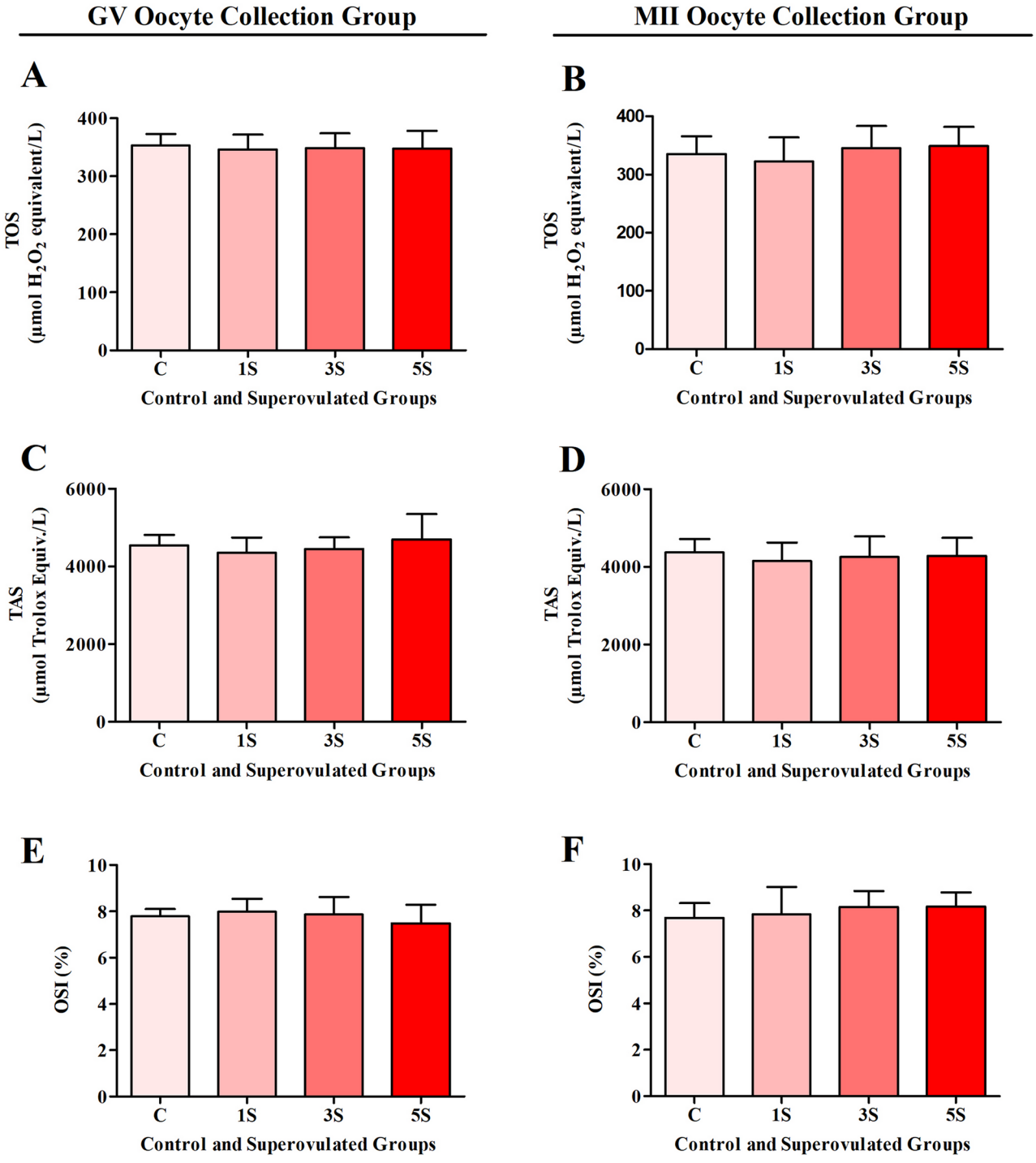


Fig. 7 The total oxidant status (TOS), antioxidant status (TAS), and oxidative stress index (OSI) in serum samples of the control and superovulated groups. (**A**) The TOS levels in GV oocyte- and (**B**) MII oocyte-obtained groups. We found no significant differences between the groups. (**C**) The TAS levels in GV oocyte- and (**D**) MII oocyte-obtained groups. No statistical significance existed between the groups. (**E**) The OSI percentages of GV oocyte- and (**F**) MII-oocyte obtained groups. No difference was noted between the groups. Differences were analyzed by one-way ANOVA and Tukey's post hoc test. Data are presented as mean ± standard deviation (SD). $P < 0.05$ was considered statistically significant. C, control; S, superovulated

in the 3S group. The relative decrease in *Tert* mRNA levels in the 3S group compared to the other groups suggests that the initial rise following a single superovulation was sufficient to achieve adequate TERT protein levels, thereby eliminating the need for further increases. However, consecutive PMSG injections increased again in the 5S group, which may be associated with maintaining this level and regulating the decrease in *Tert* mRNA. Since

PMSG, as an FSH analogue, increases the number of follicles that produce estradiol in high amounts and also progesterone, the elevated *Tert* mRNA levels could be due to the increased estradiol and progesterone levels, which subsequently led to enhanced *Tert* mRNA levels [15, 17]. As granulosa cells of follicles constitutively express FSH receptors after gonadotropin-dependent stages, these cells secrete estrogen and progesterone when stimulated with FSH or PMSG in vitro [23, 45]. Thus, although we found no remarkable differences in serum estradiol and progesterone levels in the superovulated groups, these hormone levels may be altered in follicular microenvironment, which might be associated with the *Tert* mRNA fluctuations.

In MII oocytes, *Tert* mRNA reached the highest level in the 1S group. This effect may be due to enhanced estradiol levels in microenvironment of this group because there may be more growing follicles than in the 3S and 5S groups. We suppose that the 3S and 5S groups may have undergone more follicular loss due to a round of gonadotropin treatments, which resulted in reduced estradiol levels. The decreased *Tert* levels in the 3S and 5S groups showed that MII oocytes brought this increase to normal levels possibly by unknown intracellular regulations.

In the current study, we found higher estradiol and progesterone concentrations in the mice from which GV oocytes were retrieved. These increases possibly resulted from elevated numbers of growing follicles secreting these hormones after being treated with PMSG. In contrast, we determined a decrease in estradiol levels in the superovulated groups from which MII oocytes were obtained, as reported in a previous study [9]. The ovulation of many oocytes and depletion of growing follicles dependent on repeated superovulation may lead to reduced estradiol levels. On the other hand, progesterone levels in MII oocyte-collected superovulated groups increased possibly due to enhanced corpus luteum formation following consecutive ovulations. It is well-known that corpora lutea are able to secrete progesterone hormone at high levels.

Another remarkable finding of the current study is to observe POFs in the ovaries of mice from which GV oocytes were collected [46]. Repeated PMSG injections in the 3S and 5S groups resulted in maintaining estradiol at high levels. Elevation of estradiol and decrease of progesterone levels are associated with formation of POFs [46, 47]. It is important to note that POFs usually appear during fetal development, but rarely in adult periods [48]. These structures can be formed in adult ovaries under the influences of estradiol, disruption of apoptotic pathway, certain ovarian factors, and other hormonal changes [48]. A study on porcine ovaries has shown that higher 17beta-estradiol and lower progesterone concentrations caused formation of POFs by increasing secretion of oocyte-specific factors [47]. These results support the hypothesis that hormonal changes in GV oocyte-collected groups may play a significant role in formation of POFs possibly through combination of early developing follicles.

Despite discovering important findings, this study has some limitations. We measured oxidative stress only in serum samples. Analyzing ROS levels in ovarian environment and even in oocytes following superovulation may contribute to discovering the potential relationship between oxidative stress and altered telomere length in GV and MII oocytes. Also, we have not measured telomerase activity in GV and MII oocytes to precisely understand functional implication of TERT protein levels in these oocytes. Finally, evaluating expression levels of the telomere-associated proteins responsible for telomeric integrity, such as TRF1, TRF2, and POT1, in the oocytes may contribute to explaining altered telomere length in GV and MII oocytes.

In conclusion, we observed that superovulation causes telomere shortening and increases the levels of *Terc* RNA and *Tert* mRNA in GV oocytes. In MII oocytes, while a single superovulation increases telomere length, repeated superovulation fails to maintain this increase. The current study also demonstrated that superovulation alters estradiol and progesterone levels in serum samples of mice from which GV and MII oocytes were collected. These findings may have important implications for human assisted reproductive technologies (ARTs), where repeated ovarian stimulation is commonly used. The observed changes in telomere dynamics and hormone levels suggest that repeated stimulation protocols should be carefully assessed for their potential impact on oocyte quality and reproductive outcomes. Thus, further studies are required to elucidate the molecular biological mechanisms leading to telomere length changes in GV and MII oocytes following superovulation.

Supplementary Information

The online version contains supplementary material available at https://doi.org/10.1186/s13048-025-01735-x.

Supplementary Material 1

Supplementary Material 2

Supplementary Material 3

Acknowledgements

We would like to thank Dr. Zeynep Ozturk (PhD) and Gizem Korkmaz (MSc) for helping in ELISA, TAS, and TOS analyses as well as the Central Laboratory in Akdeniz University Hospital for giving permission to use the RT-qPCR machine. Additionally, we thank Dilara Onemli (MSc student) for her help in creating Supplementary Material 3.

Author contributions

SO and BT designed the study. BT, GT, and YB collected GV and MII oocytes. BT, GT, and YB performed immunofluorescence, ELISA, and RT-qPCR experiments.

BT measured TAS and TOS levels and performed qPCR. BT analyzed all data and wrote the manuscript. GT and YB read the manuscript. SO evaluated all the experimental results, managed the investigation, and critically read and revised the manuscript.

Funding
This study was supported by TUBITAK (Projects no. 221S182 and 223S591) and Akdeniz University Research Fund (Project no. TYL-2022-5826).

Data availability
No datasets were generated or analysed during the current study.

Declarations

Ethics approval and consent to participate
All experimental protocols were performed in accordance with relevant guidelines and regulations approved by the Akdeniz University Institutional Animal Care and Use Committee (Protocol no. 1312/2021.05.24).

Consent for publication
Not applicable.

Competing interests
The authors declare no competing interests.

Received: 20 March 2025 / Accepted: 23 June 2025
Published online: 29 September 2025

References

1. Lee M, et al. Adverse effect of superovulation treatment on maturation, function and ultrastructural integrity of murine oocytes. Mol Cells. 2017;40(8):558–66.
2. Ertzeid G, Storeng R. The impact of ovarian stimulation on implantation and fetal development in mice. Hum Reprod. 2001;16(2):221–5.
3. Ertzeid G, Storeng R. Adverse effects of gonadotrophin treatment on pre- and postimplantation development in mice. J Reprod Fertil. 1992;96(2):649–55.
4. Van der Auwera I, D'Hooghe T. Superovulation of female mice delays embryonic and fetal development. Hum Reprod. 2001;16(6):1237–43.
5. Chao HT, et al. Repeated ovarian stimulations induce oxidative damage and mitochondrial DNA mutations in mouse ovaries. Ann N Y Acad Sci. 2005;1042:148–56.
6. Xiao P, et al. Melatonin alleviates the deterioration of oocytes from mice subjected to repeated superovulation. J Cell Physiol. 2019;234(8):13413–22.
7. Kalthur G, et al. Distribution pattern of cytoplasmic organelles, spindle integrity, oxidative stress, octamer-binding transcription factor 4 (Oct4) expression and developmental potential of oocytes following multiple superovulation. Reprod Fertil Dev. 2016;28(12):2027–38.
8. Miyamoto K, et al. Effect of oxidative stress during repeated ovulation on the structure and functions of the ovary, oocytes, and their mitochondria. Free Radic Biol Med. 2010;49(4):674–81.
9. Wang Q et al. Repeated superovulation accelerates primordial follicle activation and Atresia. Cells, 2022. 12(1).
10. Nie X, et al. Establishment of a mouse model of premature ovarian failure using consecutive superovulation. Cell Physiol Biochem. 2018;51(5):2341–58.
11. Shammas MA. Telomeres, lifestyle, cancer, and aging. Curr Opin Clin Nutr Metab Care. 2011;14(1):28–34.
12. Barnes RP, Fouquerel E, Opresko PL. The impact of oxidative DNA damage and stress on telomere homeostasis. Mech Ageing Dev. 2019;177:37–45.
13. Ozturk S, Sozen B, Demir N. Telomere length and telomerase activity during oocyte maturation and early embryo development in mammalian species. Mol Hum Reprod. 2014;20(1):15–30.
14. Tire B, Ozturk S. Potential effects of assisted reproductive technology on telomere length and telomerase activity in human oocytes and early embryos. J Ovarian Res. 2023;16(1):130.
15. Taheri M, et al. Hormonal regulation of telomerase activity and hTERT expression in steroid-regulated tissues and cancer. Cancer Cell Int. 2022;22(1):258.
16. Toupance S et al. Ovarian telomerase and female fertility. Biomedicines, 2021. 9(7).
17. Bayne S, et al. Estrogen deficiency reversibly induces telomere shortening in mouse granulosa cells and ovarian aging in vivo. Protein Cell. 2011;2(4):333–46.
18. Kyo S, et al. Estrogen activates telomerase. Cancer Res. 1999;59(23):5917–21.
19. Vidal JD, et al. Estrogen replacement therapy induces telomerase RNA expression in the macaque endometrium. Fertil Steril. 2002;77(3):601–8.
20. Zheng Q, Huang J, Wang G. Mitochondria, telomeres and telomerase subunits. Front Cell Dev Biol. 2019;7:274.
21. Lin J, Epel E. Stress and telomere shortening: insights from cellular mechanisms. Ageing Res Rev. 2022;73:101507.
22. Zhang S, et al. Repeated controlled ovarian stimulation-induced ovarian and uterine damage in mice through the PI3K/AKT signaling pathway. Hum Cell. 2023;36(1):234–43.
23. Mordechai A, et al. Increasing telomerase enhanced steroidogenic genes expression and steroid hormones production in rat and human granulosa cells and in mouse ovary. J Steroid Biochem Mol Biol. 2020;197:105551.
24. Berteli TS, et al. Impact of superovulation and in vitro fertilization on LINE-1 copy number and telomere length in C57BL/6 J mice blastocysts. Mol Biol Rep. 2022;49(6):4909–17.
25. Tang SB, et al. Multiple superovulations alter histone modifications in mouse early embryos. Reproduction. 2019;157(6):511–23.
26. Ozturk S. Selection of competent oocytes by morphological criteria for assisted reproductive technologies. Mol Reprod Dev. 2020;87(10):1021–36.
27. Lemseffer Y et al. Methods for assessing oocyte quality: A review of literature. Biomedicines, 2022. 10(9).
28. Doeing DC, Borowicz JL, Crockett ET. Gender dimorphism in differential peripheral blood leukocyte counts in mice using cardiac, tail, foot, and saphenous vein puncture methods. BMC Clin Pathol. 2003;3(1):3.
29. Yamada-Fukunaga T, et al. Age-associated telomere shortening in mouse oocytes. Reprod Biol Endocrinol. 2013;11:108.
30. Callicott RJ, Womack JE. Real-time PCR assay for measurement of mouse telomeres. Comp Med. 2006;56(1):17–22.
31. Uysal F, Ozturk S, Akkoyunlu G. Superovulation alters DNA methyltransferase protein expression in mouse oocytes and early embryos. J Assist Reprod Genet. 2018;35(3):503–13.
32. Uysal F, Ozturk S. Embryonic poly(A)-binding protein is differently expressed and interacts with the messenger RNAs in the mouse oocytes and early embryos. J Cell Biochem. 2019;120(3):4694–709.
33. Ozturk S, Sozen B, Demir N. Epab and Pabpc1 are differentially expressed in the postnatal mouse ovaries. J Assist Reprod Genet. 2015;32(1):137–46.
34. Talibova G, Bilmez Y, Ozturk S. Increased double-strand breaks in aged mouse male germ cells May result from changed expression of the genes essential for homologous recombination or nonhomologous end joining repair. Histochem Cell Biol. 2023;159(2):127–47.
35. Bilmez Y, Talibova G, Ozturk S. Expression of the histone lysine methyltransferases SETD1B, SETDB1, SETD2, and CFP1 exhibits significant changes in the oocytes and granulosa cells of aged mouse ovaries. Histochem Cell Biol. 2022;158(1):79–95.
36. Aykal MB, et al. Effects of boric acid as maternal feed additives on the development and sex ratio of mouse pups. Biol Trace Elem Res; 2024.
37. Alm H, et al. Occurrence of polyovular follicles in mouse lines selected for high fecundity. J Reprod Dev. 2010;56(4):449–53.
38. Xie H, et al. Roles of gonadotropins and meiosis-activating sterols in meiotic resumption of cultured follicle-enclosed mouse oocytes. Mol Cell Endocrinol. 2004;218(1–2):155–63.
39. Longobardi S et al. Gonadotropin activity during early folliculogenesis and implications for polycystic ovarian syndrome and premature ovarian insufficiency: A narrative review. Int J Mol Sci, 2024. 25(14).
40. De Rosa M, Johnson SA, Opresko PL. Roles for the 8-Oxoguanine DNA repair system in protecting telomeres from oxidative stress. Front Cell Dev Biol. 2021;9:758402.
41. Bayne S, et al. Estrogen deficiency leads to telomerase inhibition, telomere shortening and reduced cell proliferation in the adrenal gland of mice. Cell Res. 2008;18(11):1141–50.
42. Shin YA, Lee KY. Low Estrogen levels and obesity are associated with shorter telomere lengths in pre- and postmenopausal women. J Exerc Rehabil. 2016;12(3):238–46.
43. Kosebent EG, Uysal F, Ozturk S. The altered expression of telomerase components and telomere-linked proteins May associate with ovarian aging in mouse. Exp Gerontol. 2020;138:110975.

44. Zhang J, et al. Repeated superovulation increases the risk of osteoporosis and cardiovascular diseases by accelerating ovarian aging in mice. Aging. 2018;10(5):1089–102.
45. Keren-Tal I, et al. Establishment of steroidogenic granulosa cell lines expressing follicle stimulating hormone receptors. Mol Cell Endocrinol. 1993;95(1–2):R1–10.
46. Reynaud K, et al. IGF system and ovarian folliculogenesis in dog breeds of various sizes: is there a link? J Endocrinol. 2010;206(1):85–92.
47. Stankiewicz T, Blaszczyk B, Udala J. A study on the occurrence of polyovular follicles in Porcine ovaries with particular reference to intrafollicular hormone concentrations, quality of oocytes and their in vitro fertilization. Anat Histol Embryol. 2009;38(3):233–9.
48. Silva-Santos KC, Seneda M. Multioocyte follicles in adult mammalian ovaries. Anim Reprod. 2011;8:58–67.

Publisher's note

Springer Nature remains neutral with regard to jurisdictional claims in published maps and institutional affiliations.